Korean J. Chem. Eng., **19**(6), 1106-1111 (2002)

Drying Characteristics of Millet in a Continuous Multistage Fluidized Bed

Kyong-Bin Choi, Sang-Il Park, Yeong-Seong Park*, Su-Whan Sung and Dong-Hyun Lee***,†**

Industry Furnace Research Team, KIER, Daejeon 305-343, Korea
*Department of Environmental Eng., Daejeon Univ., Daejeon 300-716, Korea
**Department of Chemical & Biomolecular Eng., KAIST, Daejeon 305-701, Korea
***Department of Chem. Eng., SKKU, Korea
(*Received 30 April 2002 • accepted 26 September 2002*)

Abstract−The effects of gas velocity, inlet gas temperature and the solid feed rate on the drying efficiency, the outlet solid moisture content, bed temperature in each stage, the outlet gas humidity and temperature in a rectangular acryl multistage fluidized bed (0.172 m×0.192 m×1.5 m-high) with a downcomer (0.04 m-I.D.) were investigated. The experiments were performed by using 1.9 mm millet particles. The final moisture contents of the solids increased with increasing the solid feed rate. The drying efficiency increased with increasing the wetted solid feed rate but decreased with increasing the inlet gas temperature. The drying performance of the multistage fluidized bed was compared with the single-stage fluidized bed and found to be superior under identical operation conditions. The model predicted values were well matched with the experimental data in the multistage fluidized bed dryer.

Key words: Multistage Fluidized Beds, Drying Characteristics, Drying Efficiency, Millet, Downcomer

INTRODUCTION

Drying in fluidized beds is an important thermal process removing water or liquid from moist solid particles [Palancz, 1983]. The analysis of the drying phenomenon in fluidized beds is more complicated than that of heat or mass transfer alone [Lee and Kim, 1999]. Different mechanisms control the constant- and falling rate drying regimes that can be observed successively in the drying operation [Kunii and Levenspiel, 1991].

Fluidized beds are advantageously used for drying granular materials, such as grains, fertilizers, and chemicals, as they offer large transfer areas between the phases, improved heat and mass transfer between the phases, high degree of mixing of the materials, ease of the handling and transferring of the fluidized materials, fluids with negligible temperature and concentration gradients within the bed, and suitability for the large scale operations. However, some of the disadvantages of the fluidized beds are non-adaptability to the countercurrent operation, absence of thermal and concentration gradients along the column when desired, and high degree mixing of materials resulting often in non-uniform product quantities [Kannan and Subramanian, 1998]. These disadvantages can be overcome by the use of perforated plates which configure the multistage fluidized beds.

Multistage fluidized beds have many advantages such as facilitating countercurrent action of the phases and improving the axial mixing for solid and fluid, limiting formation and growth of bubbles within the bed as compared to single stage fluidized beds. Papadatos et al. [1975] investigated the solids holdup in a multistage fluidized bed operating in continuous regime with activated carbon, varying the solids feed rate and the downcomer diameter. They proposed that the solid holdup in a multistage fluidized bed is a function of the column diameter, gas velocity, particle size, solids feed rate, weir diameter and weir height. Eleftheriades and Judd [1978] studied the gas velocity range in which the solid regime in the standpipe was a moving bed, varying both gas velocity and solid flow rate. They reported the solid mass flux necessary for moving bed regime is nearly 30 kg/m^2/s when the gas velocity is close to the minimum fluidization velocity. The solid mass flux increased up to 200 kg/m^2/s with increasing the gas velocity to maintain the moving bed regime. The maximum value varied slightly with the geometric size of the downcomer. Kannan et al. [1994] carried out a study on the range of the operating gas velocity for the multistage fluidized beds with and without downcomers. They pointed out two operating gas velocities: (1) the critical velocity, U_{cr} at which the downcomer solids level is at its maximum and they begin to transfer downwards from stage to stage, (2) the flooding velocity, U_{fd}, when the downcomer solids height is at its minimum and the solids height starts to increase indicating flooding. Kannan and Subramanian [1998] reported that the drying performance of the multistage fluidized beds with downcomers was better than that of the batch fluidized bed. The performance of the multistage fluidized beds with downcomers was also compared with the multistage fluidized beds without downcomers and found to be superior under identical operation conditions.

In the present study, the effects of gas velocity (0.032 to 0.038 Nm^3/sec), inlet gas temperature (37 to 65 °C) and solid feed rate (2.1×10^{-3} to 5.4×10^{-3} kg-dry solid/sec) on the drying characteristics of millet particles in the multistage fluidized beds were investigated. Also, the drying performance of the multistage fluidized beds was compared with the single-stage fluidized beds and the model predicted values were compared with the experimental data obtained from the multistage fluidized bed dryer.

MODELING

In this section, we will develop a model to describe the drying

†To whom correspondence should be addressed.
E-mail: dhl0128@yurim.skku.ac.kr
‡This paper is dedicated to Professor Dong Sup Doh on the occasion of his retirement from Korea University.

characteristics of the multistage fluidized beds. The residence time distribution derived from the material balance equations and the batch drying curve of Kannan et al. [1994] are used to estimate the solid concentration at each stage.

1. Material Balance Equations

The following material balance equation can be directly applied for the first stage:

$$M_s\frac{dC_1(t)}{dt} = F_sC_s(t) - F_sC_1(t) \tag{1}$$

where, M_s is the mass of the solid in the first stage. F_s is the flow rate of the solids. $C_s(t)$ and $C_1(t)$ are the concentrations of the solid in the influent stream and in the effluent stream at the first stage, respectively. Since the height of the first stage is a half of other stages, material balance equations for the other stages are as follows:

$$2M_s\frac{dC_i(t)}{dt} = F_sC_{i-1}(t) - F_sC_i(t),\ i=2,\ 3,\ 4,\ 5 \tag{2}$$

2. Residence Time Distribution

From the material balance equations of (1) and (2), we can directly derive the following residence time distribution for the first stage:

$$R_1(t) = \frac{F_s}{M_s}\exp(-F_st/M_s) \tag{3}$$

and for other stages:

$$R_2(t) = \Lambda = R_5(t) = \frac{F_s}{2M_s}\exp(-F_st/2M_s) \tag{4}$$

Here, note that Eqs. (3) and (4) represent the concentration distributions when the impulse is entered at the influent of each stage. For example, $R_5(t)$ is the concentration distribution when the impulse is entered at the effluent of the 4th stage (rather than the influent stream of the column).

3. Batch Drying Curve

The average moisture content in the particles is given by [Kannan et al., 1994] as follows.

$$\frac{C_{batch}(t)-C_{eq}}{C_{initial}(t)-C_{eq}} = \sum_{i=1}^{\infty}\frac{6Bi_m^2\exp(-\beta_i^2D_{eff}t/R_s^2)}{\beta_i^2(\beta_i^2+Bi_m^2-Bi_m)} \tag{5}$$

where β_n's are the roots of the equation.

$$\beta_i\cot(\beta_i)+Bi_m-1=0,\ i\pi<\beta_i<(i+1)\pi$$

Based on the experimental data in the fluidized bed dryer, an attempt is made to empirically relate the equilibrium moisture contents of millet with temperature as follows:

$$C_{eq} = 1.72\times10^{-7}\exp(3890/T) \tag{6}$$

The dependency of the effective diffusivity, D_{eff} on the temperature of the heating medium is well known, and its dependency on the initial moisture content has been reported for the drying solids [Chu and Hustrulid, 1968; Kameoka et al., 1986; Kannan et al., 1994]. Based on the structure proposed by Kannan et al. [1994], the effective diffusivity for the millet can be expressed as follows:

$$D_{eff} = K_aC_{initial}^{-0.13}\exp(-E_{eff}/T) \tag{7}$$

where the parameters of K_a and E_{eff} will be optimized from the experimental data sets. K_y in Eq. (5) may be obtained by using the following equation [Richardson and Szekely, 1961]:

$$\frac{2K_yR_s}{D_m} = 0.37Re^{1.18} \text{ for } 0.1<Re<15$$
$$= 2.01Re^{0.5} \text{ for } 15\le Re<250 \tag{8}$$

4. Estimating of the Solid Concentration for Each Stage

Now, we can estimate the solid concentration using the following equation:

$$C_i = C_{i-1}\int_0^{\infty}R_i(t)C_{batch}(t)dt \tag{9}$$

where, C_i is the steady-state concentration at the i-th stage.

5. Optimizing the Adjustable Parameters

We have derived all the necessary equations to predict the concentrations at each stage. Now, the adjustable model parameters, E_{eff} and K_a in Eq. (7) and time constant of the column ($\tau=M_s/F_s$) in Eqs. (3)-(4) should be optimized from the experiment data set. We estimated the adjustable parameters while minimizing the following cost function:

$$\min_{E_{eff},\,K_a,\,\tau}\left[V(E_{eff},\,K_a,\,\tau) = \sum_{i=1}^{5}(C_{exp}(i)-C(i))^2\right] \tag{10}$$

where, $C_{exp}(i)$ is the experiment data at the i-th stage. To solve the minimization problem, we used the Levenberg-Marquardt method. It repeats the following equation until the parameters converge:

$$\theta(k) = \theta(k-1) - \left[\left.\frac{\partial^2V}{\partial\theta^2}\right|_{\theta=\theta(k-1)} + \alpha I\right]^{-1}\left[\left.\frac{\partial V}{\partial\theta}\right|_{\theta=\theta(k-1)}\right] \tag{11}$$

where, $\theta(k)$ is the parameters corresponding to the k-th iteration. α is a small positive value that can be updated every iteration to compromise between the robustness and the convergence rate.

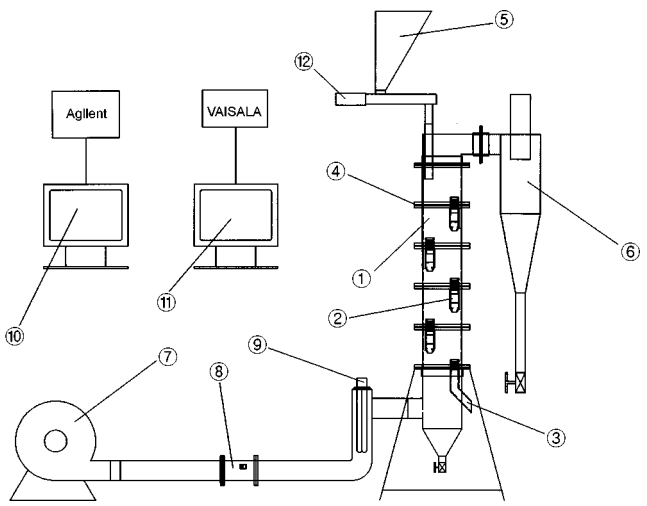

Fig. 1. Experimental setup of a multistage fluidized bed dryer.

1. Main column
2. Downcomer
3. Discharge port
4. Perforated plate
5. Hopper
6. Cyclone
7. Blower
8. Turbine flowmeter
9. Heater
10. Data logger for temperature
11. Data logger for humidity
12. Screw feeder

Table 1. Ranges of experimental variables

No.	Variable	Unit	Operating ranges
1	Gas temperature	°C	37, 48, 54, 65
2	Solid feed rate	kg dry solid/sec	2.1×10^{-3}, 3.4×10^{-3}, 4.4×10^{-3}, 5.4×10^{-3}
3	Gas flow rate	Nm^3/sec	0.032 (U_g/U_{mf}=1.90), 0.038 (U_g/U_{mf}=2.14)

$$\theta = [E_{eff} K_a \tau]^T \quad (12)$$

$$\frac{\partial V}{\partial \theta} = \left[\frac{\partial V}{\partial E_{eff}} \frac{\partial V}{\partial K_a} \frac{\partial V}{\partial \tau}\right]^T \quad (13)$$

EXPERIMENTAL

Drying experiments using 1.9-mm millet (ρ_s=1,350 kg/m^3, angularity=1.1, U_{mf}=0.70 m/s) were carried out in a 0.0243 m^2×1.5 m-high acryl column shown in Fig. 1. The height of each stage of the multistage fluidized bed was 0.2 m. The experimental setup consisted of a fluidization column with a provision to continuously feed and discharge material at a controlled rate. For the multistage fluidized bed with downcomers, the perforated plates have 3 mm×188 perforations with 4% opening ratio, and 0.04 m-I.D. downcomer on the periphery is used to discharge the millets. The solid bed height is 0.02 m in the first stage and 0.04 m in other stages. The height of each stage in the multistage fluidized bed would be controlled by the height of the downcomer. The ranges of the experimental variables are listed in Table 1. Air at the desired temperature was introduced at the bottom of the multistage bed. The millets were fed into the top stage. The temperatures of the heating medium in each stage were noted by the thermocouples. The moisture content of the materials was determined by the moisture analyzer (KETT electric Lab., FD-620). Air humidity was determined by the humidity sensor (Vaisala Co., HMP235). For the fluidized bed dryer, energy is required to evaporate the moisture, and thus, the energy loss with the exit air streams dominates the energy demand of a dryer. Drying efficiency of a dryer, η, can be described by the following equation [Lee and Kim, 1994].

$$\eta = \frac{H_2 - H_1}{H_w - H_1} \quad (14)$$

where H_1, H_2 and H_w are inlet gas humidity, outlet gas humidity and saturated humidity at inlet gas condition, respectively.

RESULTS AND DISCUSSION

In Fig. 2, the diagram of the multistage fluidized bed dryer is presented together with the experimental data. As can be seen, operating variables such as the inlet moisture content, inlet gas temperature and gas flow rate were set at 0.202 kg H_2O/kg dry solid, 48 °C and 0.038 Nm^3/sec, respectively. The solid moisture content of the first stage was higher than that of the fifth stage because the wetted solids were fed into the top of the multistage fluidized bed dryer. Also, the hot gas temperature of the first stage was lower than that of the fifth stage since the heat of the inlet gas was consumed during the evaporation of the moisture in the wetted solids. The absolute humidity of the inlet hot gas before the drying process was 0.0034 kg H_2O/kg dry air and that of the outlet hot gas after the drying process was 0.0096 kg H_2O/kg dry air. Note that all the experimental data given in Fig. 2 are the steady state values.

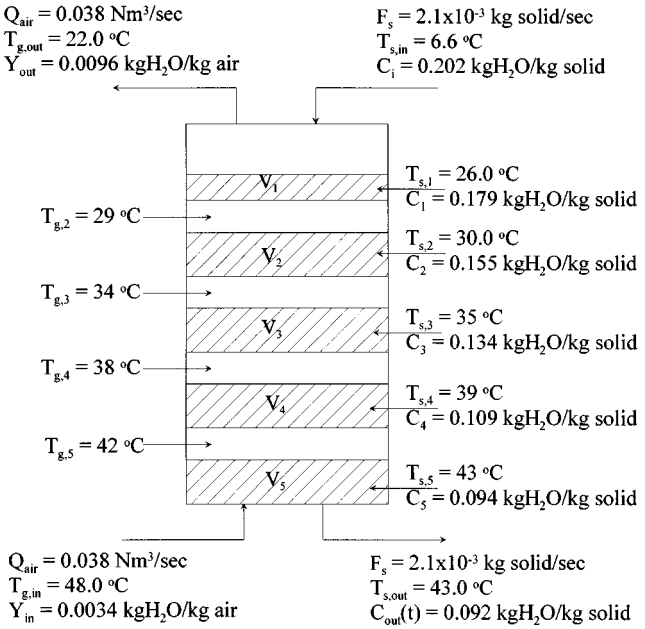

Fig. 2. Diagram of the multistage fluidized bed dryer.

The influence of the various process parameters, such as the temperature of the inlet gas, flow rate of the inlet gas, flow rate of the wetted solids, and number of stages, is studied for the multistage fluidized beds. The variation of the bed temperature in each stage at a constant inlet gas temperature (48 °C) is shown in Fig. 3 as a function of time elapsed after start-up. As can be seen in Fig. 3, the bed temperature in each stage initially increased sharply and grad-

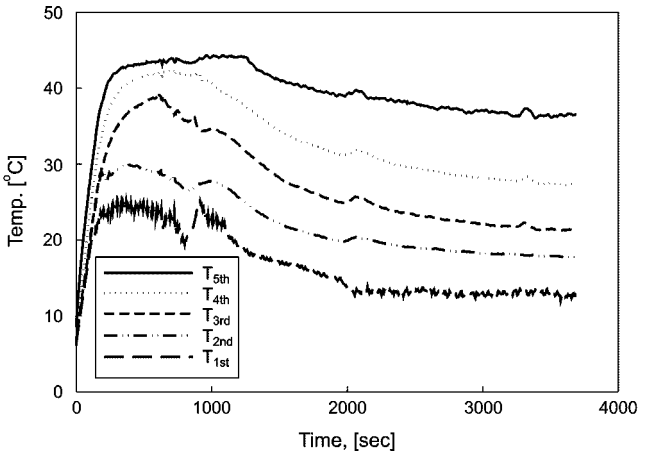

Fig. 3. Variation of bed temperature in each stage as a function of time elapsed after startup.

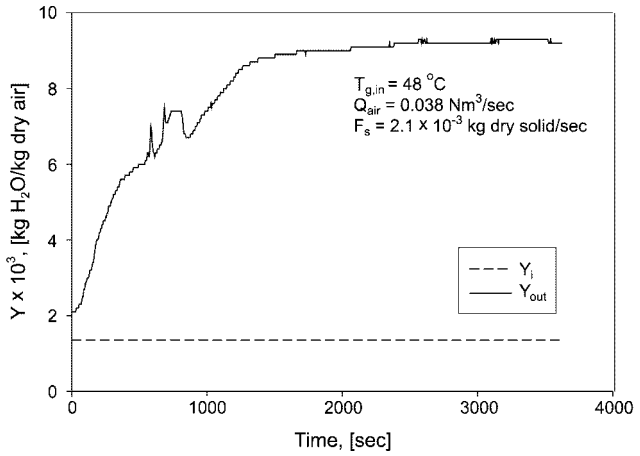

Fig. 4. Variation of outlet gas humidity as a function of time elapsed after startup.

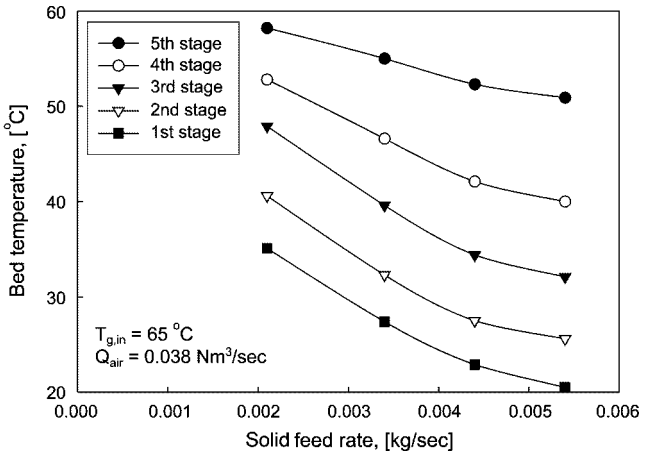

Fig. 6. Effect of the solid feed rate on the bed temperature of each stage in the multistage fluidized beds.

ually decreased with drying time and then reached a constant value. Approximately 2000 seconds were needed to reach the steady state in the present system. At the steady state, the bed temperature of the fifth stage was higher than that of the first stage since the fifth stage was located higher than hot gas distributor and the first stage lower than the solid feeding chamber.

The variation of the outlet gas humidity at a constant inlet gas temperature (48 °C) is shown in Fig. 4. The dotted line represents the inlet gas humidity. As seen, the outlet gas humidity gradually increased with drying time and then reached a constant value.

The effect of the solid feed rate on the ratio of the solid moisture content of each stage in the five-stage fluidized beds is shown in Fig. 5. As can be seen, the ratio of the solid moisture content of every stage increased with increasing the solid feed rate due to the inrease of the wet solids at the constant inlet temperature and hot gas flow rate. As known, the solid moisture content of the first stage was higher than that of the fifth stage since the mean residence time of the fifth stage was longer than that of the first stage.

The effect of the solid feed rate on the bed temperature of each stage in the multistage fluidized beds is shown in Fig. 6, whereby the bed temperature decreased with increasing the flow rate of the wetted solids. There was a drop in bed temperature from the fifth stage to the first stage that was smaller for the lower feed rate of the wetted solids. The drop of bed temperature increased with an increase in the solid feed rate. Note that an increase in the solid feed rate actually decreased the solids mean residence time. It can be inferred from the fifth stage that the lower the residence time of the solids and the higher the feed temperature of the air, the greater was the temperature drop from the first stage to the fifth stage of the multistage fluidized bed dryer. With a long mean residence time, the materials not only stayed for a longer time in the bed but were also subjected to a higher temperature within the bed in all stages.

The effect of the solid feed rate on the drying efficiency within the range of the inlet gas temperature (37-65 °C) in the multistage stage of fluidized bed dryer is shown in Fig. 7. As can be seen in Fig. 7, the drying efficiency increased with increasing solid feed rate due to the increase of the outlet gas humidity. However, the drying efficiency decreased with increasing the inlet gas temperature. Lee and Kim [1994] reported that the drying efficiency increased with increasing the moisture feed rate but decreased with increasing the inlet gas temperature and the inlet gas velocity. Nakagawa et al. [1992] also reported similar results. Recently, Shin et al. [2000]

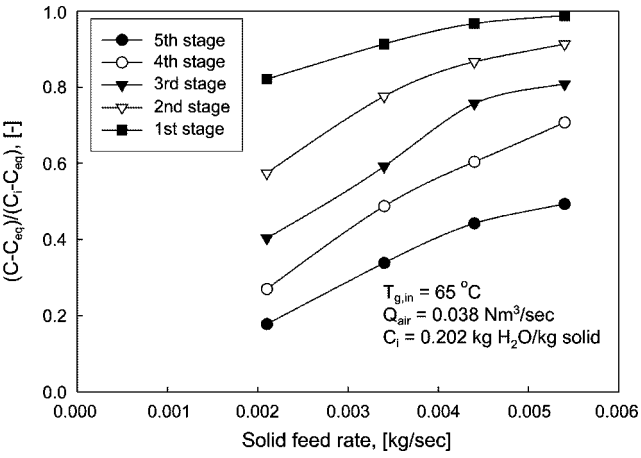

Fig. 5. Effect of the solid feed rate on the ratio of the solid moisture content of each stage in the multistage fluidized beds.

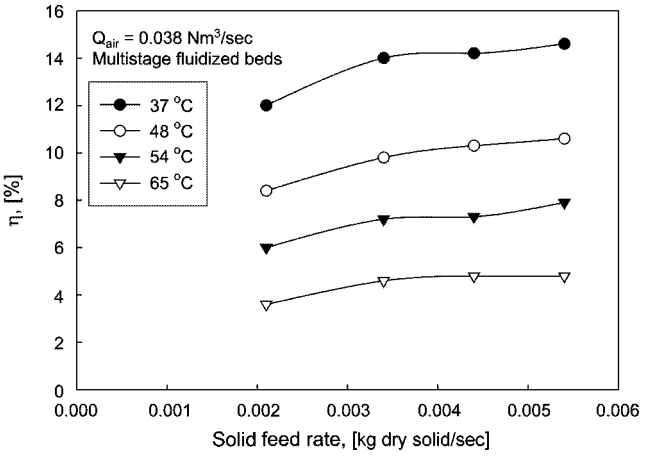

Fig. 7. Effect of the solid feed rate on the drying efficiency in the multistage stage of fluidized bed dryer.

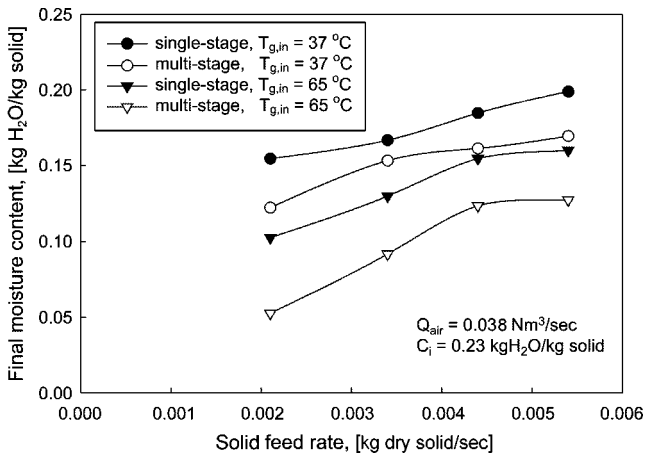

Fig. 8. Comparison of the performance of the single-stage and multistage fluidized bed.

reported that the drying efficiency decreased with increasing the inlet gas temperature and relatively insensitive to superficial gas velocity and increased with feed rate of sludge.

Fig. 8 compares the performance of the single-stage and multistage fluidized beds based on the solid feed rate. It is known that an increase in the solid feed rate actually decreases the mean residence time of solids. Therefore, the final moisture contents of the solids increase with increasing the solid feed rate due to shortening the mean residence time. As can be seen in Fig. 8, the drying performance of the multistage fluidized bed was better than that of a single stage fluidized bed due to the narrow residence time distribution in the multistage fluidized beds, although the mean residence time of both single-stage and multistage fluidized beds was the same. As reported by Kannan and Subramanian [1998], the drying performance of the multistage fluidized beds was better than that of the batch fluidized bed.

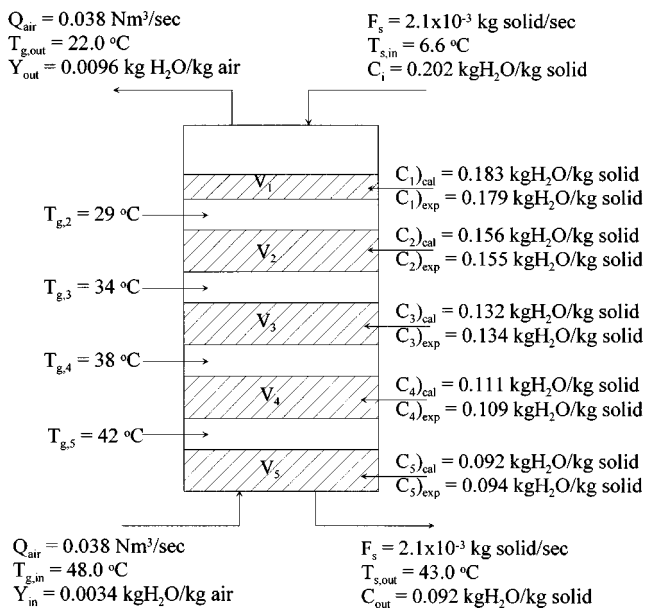

Fig. 9. Comparison of the experimental data with the model predictions using the present model.

The model was developed to describe the drying characteristics of the multistage fluidized beds. The residence time distribution derived from the material balance equations and the batch drying curve of Kannan et al. [1994] were used to estimate the solid moisture concentration at each stage. The model predicted values of the solid moisture content are shown in Fig. 9 with the data obtained experimentally in the multistage fluidized bed. As can be seen in Fig. 9, the model predicted values were well matched with the experimental data. The adjustable parameters--the effective activation energy, K_a and mean residence time--were optimized from the experimental data set using the Levenberg-Marquardt method. The values of E_{eff}, K_a and τ in this case were 2,000 kJ/mol, 5.8×10^{-7} and 120 sec, respectively.

CONCLUSION

The effects of the gas velocity, the inlet gas temperature and the solid feed rate on the drying efficiency, the outlet solid moisture content, the bed temperature in each stage, the outlet gas humidity and temperature have been determined in a (0.0243 $m^2\times1.5$ m-high) rectangular acryl multistage fluidized bed with a downcomer. The model was developed to describe the drying characteristics of the multistage fluidized beds. The residence time distribution derived from the material balance equations and the batch drying curve of Kannan et al. [1994] were used to estimate the solid moisture concentration at each stage.

The final moisture contents of the solids increased with increasing the solid feed rate. The drying efficiency increased with increasing the wetted solid feed rate but decreased with increasing the inlet gas temperature. The drying performance of the multistage fluidized bed was compared with the single-stage fluidized bed and found to be superior under identical operation conditions. The model predicted values were well matched with the experimental data in the multistage fluidized bed dryer.

ACKNOWLEDGMENT

We acknowledge a grant-in-aid (2000-E-ID01-P-04) for research from Ministry of Commerce Industry and Energy.

NOMENCLATURE

Bi_m : Biot number [-]
C_{eq} : equilibrium moisture content [kg H_2O/kg dry solid]
C_{exp} : experimental solid moisture content [kg H_2O/kg solid]
C_i : initial solid moisture content,[kg H_2O/kg dry solid]
$C_1(t)$: moisture content of the solid in the effluent stream [kg H_2O/kg solid]
$C_s(t)$: moisture content of the solid in the influent stream [kg H_2O/kg solid]
D_{eff} : effective diffusivity [m/s^2]
D_m : molecular diffusivity [m/s^2]
E_{eff} : effective activation energy [kJ/mole]
F_s : flow rate of the solids [kg/sec]
H_1 : inlet gas humidity [kg H_2O/kg dry air]
H_2 : outlet gas humidity [kg H_2O/kg dry air]
H_w : saturated humidity at inlet gas condition [kg H_2O/kg dry air]

I : unit matrix [-]
K_a : adjustable parameter in Eq. (7) [-]
K_y : mass transfer coefficient across particle surface [m/s]
M_s : mass of the solid [kg]
Q_{air} : gas flow rate [Nm^3/sec]
Re : Reynolds number [-]
$R_i(t)$: residence time distribution [-]
R_s : radius of millet [m]
T_b : bed temperature [°C]
T : time [sec]
$T_{g,out}$: outlet gas temperature [°C]
T_s : solid temperature [°C]
U_g : superficial gas velocity [m/s]
Y_{in} : inlet gas humidity [kg H_2O/kg dry air]
Y_{out} : outlet gas humidity [kg H_2O/kg dry air]

Greek Letters

η : drying efficiency [-]
τ : time constant [sec]
$\theta(k)$: parameter corresponding to the k-th iteration in Eq. (11) [-]
β_n : roots of the equation in Eq. (5) [-]

REFERENCES

Chu, S. T. and Hustrulid, A., "Numerical Solution of Diffusion Equation," *Trans ASAE*, **11**, 705 (1968).

Eleftheriades, C. M. and Judd, M. R., "The Design of Downcomers Joining Gas-fluidized Beds in Multistage Systems," *Powder Technol.*, **21**, 217 (1978).

Kameoka, T., Hosokawa, A. and Morishima, H., "Simulation of Heat and Mass Transfer during through-Drying Process of Rough Rice," Drying of Solids: Recent International Developments, Mujumdar, A. S., Ed., Halstad Press, New York (1986).

Kannan, C. S., Rao, S. S. and Verma, Y. B. G., "A Kinetic Model for Drying of Solids in Batch Fluidized Beds," *Ind. Eng. Chem. Res.*, **33**, 363 (1994).

Kannan, C. S. and Subramanian, N. B., "Some Drying Aspects of Multistage Fluidized Beds," *Chem. Eng. Technol.*, **21**, 961 (1998).

Kunii, D. and Levenspiel, O., "Fluidization Engineering," Butterworth-Heinemann Publication, Boston (1991).

Lee, D. H. and Kim, S. D., "Drying Characteristics of PVC Resin in an Inert Medium Fluidized Bed," *HWAHAK GONGHAK*, **32**, 463 (1994).

Lee, D. H. and Kim, S. D., "Mathematical Model for Batch Drying in an Inert Medium Fluidized Bed," *Chem. Eng. Technol.*, **22**, 443 (1999).

Nakagawa, N., Ohsawa, K., Takarada, T. and Kato, K., "Continuous Drying of a Fine Particles-Water Slurry in a Powder-Particle Fluidized Bed," *J. Chem. Eng. Japan*, **25**, 495 (1992).

Palancz, B., "A Mathematical Model for Continuous Fluidized Bed Drying," *Chem. Eng. Sci.*, **38**, 1045 (1983).

Papadatos, K., Svrcek, W. Y. and Bergougnou, M. A., "Holdup Dynamics of a Single Stage Gas-Solid Fluidized Bed Absorber," *Can. J. Chem. Eng.*, **53**, 686 (1975),

Richardson, J. F. and Szekely, J., "Mass Transfer in a Fluidized Bed," *Trans. Inst. Chem. Eng.*, **39**, 212 (1961).

Shin, Y. S., Kim, H. C. and Chun, H. S., "Drying of Water Treatment Process Sludge in a Fluidized bed Dryer," *Korean J. Chem. Eng.*, **17**, 22 (2000).